

LETTER • OPEN ACCESS

## Elevated risk of tropical cyclone precipitation and pluvial flood in Houston under global warming

To cite this article: Laiyin Zhu *et al* 2021 *Environ. Res. Lett.* **16** 094030

View the [article online](#) for updates and enhancements.

You may also like

- [Tide-rainfall flood quotient: an incisive measure of comprehending a region's response to storm-tide and pluvial flooding](#)  
Mohit Prakash Mohanty, Mazhuvanchery Avarachen Sherly, Subimal Ghosh et al.
- [H<sub>2</sub>O<sub>2</sub> as a fungicide in the growth phase of green \*Haematococcus pluvialis\*](#)  
Judy Retti Witono, Valine Novianty, Y I P Arry Miryanti et al.
- [Characterizing precipitation events leading to surface water flood damage over large regions of complex terrain](#)  
Daniel Benjamin Bernet, Simona Trefalt, Olivia Martius et al.

ENVIRONMENTAL RESEARCH  
LETTERS

## LETTER

## Elevated risk of tropical cyclone precipitation and pluvial flood in Houston under global warming

## OPEN ACCESS

RECEIVED  
19 June 2021REVISED  
28 July 2021ACCEPTED FOR PUBLICATION  
17 August 2021PUBLISHED  
27 August 2021

Original content from this work may be used under the terms of the [Creative Commons Attribution 4.0 licence](#).

Any further distribution of this work must maintain attribution to the author(s) and the title of the work, journal citation and DOI.

Laiyin Zhu<sup>1</sup> , Kerry Emanuel<sup>2</sup> and Steven M Quiring<sup>3</sup><sup>1</sup> Department of Geography, Environment, and Tourism, Western Michigan University, Kalamazoo, MI, United States of America<sup>2</sup> Lorenz Center, Massachusetts Institute of Technology, Cambridge, MA, United States of America<sup>3</sup> Atmospheric Sciences Program, Department of Geography, The Ohio State University, Columbus, OH, United States of AmericaE-mail: [laiyin.zhu@wmich.edu](mailto:laiyin.zhu@wmich.edu)**Keywords:** tropical cyclone, precipitation, flood, risk, global warming, CMIP6Supplementary material for this article is available [online](#)**Abstract**

Pluvial floods generated by tropical cyclones (TCs) are one of the major concerns for coastal communities. Choosing Houston as an example, we demonstrate that there will be significantly elevated risk of TC rainfall and flood in the future warming world by coupling downscaled TCs from Model Intercomparison Project Phase 6 models with physical hydrological models. We find that slower TC translation speed, more frequent stalling, greater TC frequency, and increased rain rate are major contributors to increased TC rainfall risk and flood risk. The TC flood risk increases more than the rainfall. Smaller watersheds with a high degree of urbanization are particularly vulnerable to future changes in TC floods in a warming world.

**1. Introduction**

Tropical Cyclones (TCs) are one of the major hazards to coastal communities around the world. In the United States, TCs comprise 53.4% percent of the total cost of billion-dollar weather events from 1920 to 2020 making them one of the most expensive weather disasters in the US (NOAA 2021). Multiple Earth System Models (ESMs) and different downscaling models (Wehner *et al* 2014, Emanuel 2017, 2021, Patricola and Wehner 2018, Irvine *et al* 2019, Michaelis and Lackmann 2019, Knutson *et al* 2020) predict that anthropogenic climate change may increase the probability of the most intense TCs and their rain rate. Pluvial flood risk is further exacerbated by rapid urbanization in coastal areas (Zhu *et al* 2015, Zhang *et al* 2018).

Mismatches exist between the spatial resolution of most current ESMs and the scale of TCs (Davis 2018, Knutson *et al* 2020, Emanuel 2021). Most current ESMs have greater than 50 km spatial resolution (Emanuel 2021) while a much more granular spatial resolution is needed to capture the realistic structure of TCs and represent the most intense TCs (categories 4 and 5) (Davis 2018, Knutson *et al* 2020). Although

different downscaling approaches have been introduced (Emanuel 2013, Knutson *et al* 2013, Patricola and Wehner 2018), there are many debates on how TC will change under future climate, particularly their frequencies (Knutson *et al* 2020). Extreme precipitation is characterized by rate, frequency, and duration and they all control the magnitude of pluvial floods (Trenberth *et al* 2003). The future projection of tropical cyclone precipitation (TCP) is complicated by the possible changes in TC rain rate, frequency, translation speed, size, etc (Knutson *et al* 2020). Yet there is medium-to-high confidence that TC rain rate will increase in the future, based on multiple ESM model studies (Villarini *et al* 2014, Knutson *et al* 2015, Yoshida *et al* 2017, Gutmann *et al* 2018). Uncertainties still exist on how this change will vary spatially and how the most extreme TCP will change (Knutson *et al* 2020). In addition, the historical record provides less than 100 years of reliable rainfall data from TCs in the continental US and even shorter periods in other countries. High-resolution ESMs can only simulate TC climatology for relatively short periods for decades to 100 years due to limitations in computing resources. Both the lack of historical records and limitations in ESM-based TC predictions challenge the

robust evaluation of possible changes in the risk of extreme TCP caused by greenhouse gas emissions.

Houston is prone to all kinds of TC-related hazards but particularly pluvial flooding, because of its low elevation and rapid urbanization (Zhu *et al* 2015, van Oldenborgh *et al* 2017). In recent years, Houston has experienced significant flooding from extreme precipitation generated by Tropical Storm Allison in 2001, Hurricane Ike in 2008, and Hurricane Harvey in 2017. The rapidly growing population and urbanization in this area are increasing the number of people and properties that are at risk (Salas and Obeysekera 2014). Therefore, we choose Houston as our focus and apply the newest version of synthetic downscaling technique (SDT) and tropical cyclone rainfall (TCR) algorithms to estimate TCP climatology from eight Coupled Model Intercomparison Project Phase 6 (CMIP6) models. We compare how TCP risk changes from the 1981–2010 historical runs to the 2071–2100 worst-case scenario Shared Socioeconomic Pathway Representative Concentration Pathway 8.5 (SSP5-8.5) runs. A large sample of synthetic storms is coupled with a physics-based hydrological model to predict how TCP flood risk is projected to change in two watersheds in downtown Houston.

## 2. Methods

### 2.1. SDT and TCR algorithm

The SDT was first developed in 2006 (Emanuel *et al* 2006) and it has evolved and been improved since then (Emanuel *et al* 2006, 2008, Emanuel 2013, 2021). A strength of SDT is that it can simulate a very large sample of TCs events (i.e. tens of thousands) based on either the historical climate reanalysis data or prescribed climate conditions from Global Circulation Model simulations. This provides a more robust estimation of extreme events. The SDT starts with randomly seeding nascent cyclones across the Atlantic Ocean. These disturbances evolve according to a physical TC model controlled by the large-scale atmospheric and oceanic environment from coarse-resolution reanalysis or climate models. TC tracks are calculated from a beta-and-advection model applied to the large-scale winds, and their intensity is based on a very simple axisymmetric model coupled to a simple upper-ocean model that accounts for the mixing of cold ocean water to the surface (Emanuel *et al* 2006, Emanuel 2021). Compared with global and regional models based on fluid dynamics, the SDT is (a) computational efficient, (b) based on physics of the TCs, (c) has a very high spatial resolution, and (d) can generate a very large sample for robust risk assessment of extreme events. The SDT has been rigorously evaluated with historical observations of TCs (Emanuel *et al* 2006, Emanuel 2021) and it demonstrates very good agreement with the long term statistical distributions of TC occurrence and maximum wind speed

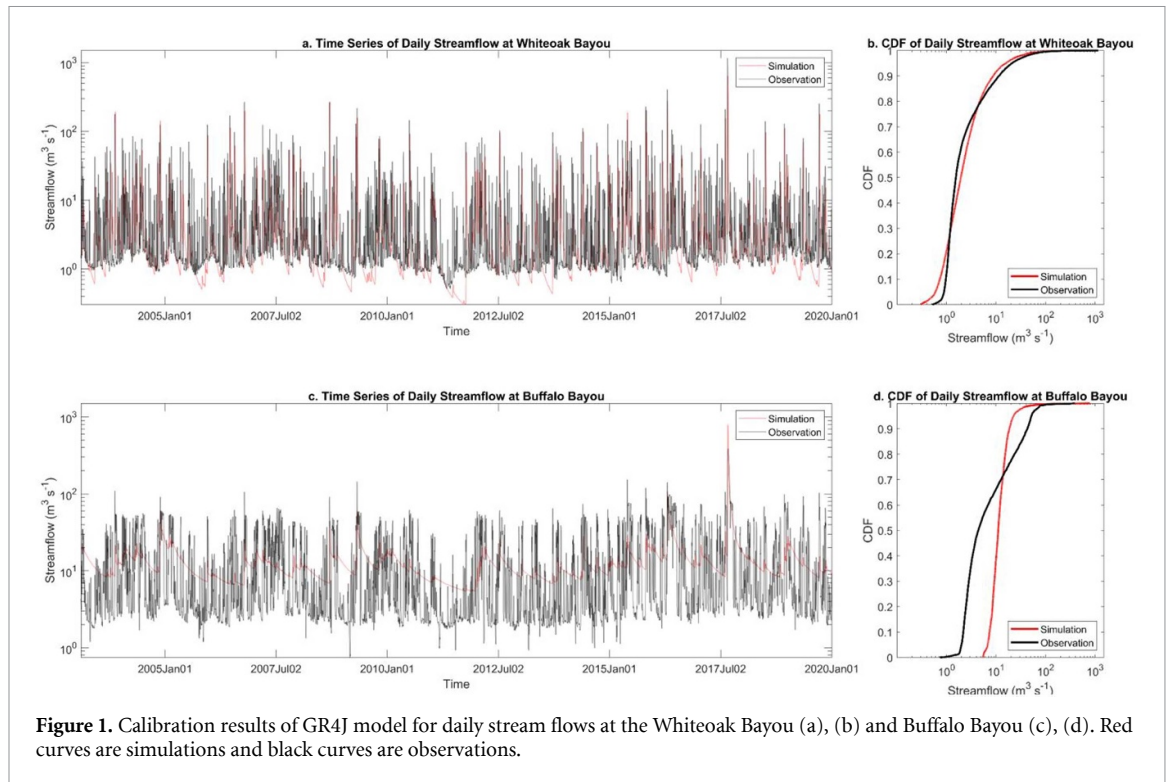
in the Atlantic Ocean recorded in the National Hurricane Center's Hurricane Databases.

The TCR algorithm was first developed in 2012 as an integral part of the SDT and routinely updated and validated. The TCR algorithm calculates the rain rate of TCs along the synthetic tracks by multiplying a precipitation efficiency with the net vertical vapor flux (Lu *et al* 2018, Feldmann *et al* 2019). It is particularly effective in simulating precipitation near the eyewall region and broad precipitation just outside the TC core (Emanuel 2017). The SDT and TCR algorithms have 2 h simulation intervals and can provide TC wind intensity and rain rate estimates at any point along the swath of generated synthetic TCs. Substantial improvements have been recently made to the TCR algorithm in recent years, including more accurate wind fields, topographical effects, more accurate representation of the surface drag and other relevant factors (Lu *et al* 2018, Feldmann *et al* 2019, Xi *et al* 2020). The TCR algorithm has been evaluated with rain gauge observations, WRF simulations, and radar observations (Zhu *et al* 2013, Lu *et al* 2018, Feldmann *et al* 2019) and its predictions agree well TCP probability distributions generated from historical observations at different locations across the US (Feldmann *et al* 2019).

We are using the most recent version of the SDT and the TCR algorithm to generate 4500 storms within 500 km of the city of Houston based on the historical climate from 1981 to 2010 and the SSP5-8.5 climate from 2071 to 2100. We select eight CMIP6 models based on the availability of specific output needed to drive the SDT and because TCs downscaled from them demonstrate good agreement with observations during the historical period. The SSP5-8.5 is a worst-case scenario, with enough emissions of greenhouse gas to produce  $8.5 \text{ W m}^{-2}$  of radiative forcing by 2100. Rain rates at 2 h intervals are estimated by the TCR and aggregated into daily and storm total rainfall for the Buffalo Bayou and Whiteoak Bayou near Houston metropolitan area. The daily TCP is used to drive our hydrological model for all 4500 storms in each of the eight models to obtain daily streamflow produced by the synthetic TCs.

### 2.2. GR4J hydrological model and model coupling

GR4J is a physics-based hydrological model that simulates the rainfall-runoff at daily time scales (Perrin *et al* 2003). GR4J is simple in structure, with only three climate variables as input to the model at every time step (Perrin *et al* 2003). Of these, the most important are rainfall depth and potential evapotranspiration. Four parameters are calibrated for each GR4J model:  $\times 1$ , the maximum capacity of the production store (mm);  $\times 2$ , the groundwater exchange coefficient (mm);  $\times 3$ , the 1 d ahead maximum capacity of the routing store (mm); and  $\times 4$ , the time base of the unit hydrograph (days). More technical details about the GR4J model development and rationale



can be found in Perrin *et al* (2003) and the open R project repository airGR (<https://cran.r-project.org/web/packages/airGR/index.html>). The GR4J model has been widely applied to hydrological modeling and operational flood forecasting for drainages at different scales (Oudin *et al* 2018, Ficchi *et al* 2019).

We calculated the daily areal precipitation for both watersheds from the daily Parameter-elevation Relationships on Independent Slopes Model product (Di Luzio *et al* 2008) at a resolution of 0.1° from 2001 to 2020 and use the basin averaged daily precipitation to drive the GR4J model. Daily streamflow records from the same period are obtained from the USGS Water Data for the Nation (<https://waterdata.usgs.gov/nwis>). The USGS 0874500 Whiteoak Bayou at Houston and the USGS 08073500 Buffalo Bayou near Addicks are the two most important drainages for floods in downtown Houston and have the most complete records for model calibration. As shown in supplementary information 1 (SI 1 (available online at [stacks.iop.org/ERL/16/094030/mmedia](https://stacks.iop.org/ERL/16/094030/mmedia))), Whiteoak Bayou is a highly urbanized drainage with an area of 246.31 km<sup>2</sup>. Buffalo Bayou is a watershed with an area of 717.43 km<sup>2</sup> and is partially controlled by two flood-control reservoirs Addicks and Baker, which were constructed in 1938 and modified subsequently. We choose 2001–2020 for model calibration because we assume the hydrological responses to extreme precipitation are stationary among our streamflow simulations. Nonstationarity does exist in the longer-term time series of streamflow records. For example, rapid urbanization in Houston has increased the likelihood of extreme floods by

introducing more impervious ground surfaces and reducing the infiltration of soil (Olivera and Defee 2007, Zhu *et al* 2015, Zhang *et al* 2018). We use the most recent hydrological record and assume that the relationship between precipitation and streamflow does not change for our risk assessment. For each model calibration, we use the 1st 500 d as the spin-up period and run the model with the remaining days. We tested different versions of AirGR (GR4J and GR6J) and different error criteria, including the root mean square error, the Nash–Sutcliffe model efficiency coefficient (NSE), King–Gupta efficiency criterion (KGE), and modified King–Gupta efficiency criterion (KGE2). The GR4J with the KGE2 criteria gives the best agreement between model predictions and observations for both watersheds. As shown by figure 1, models for both watersheds show decent agreement in both time series and the cumulative probability distributions of stream flows.

The Whiteoak Bayou has better agreement than the Buffalo Bayou because the Buffalo Bayou has flood control reservoirs upstream that makes model parameter estimation more difficult. In particular, both models capture most of the extreme values in the time series. This allows us to model the probabilities of extreme stream flows generated by thousands of synthetic TCs.

The GR4J has three climatic input variables: temperature, potential evaporation (calculated from temperature and radiation), and precipitation, besides the physical characteristics of the watershed (e.g. area and topography). For each set of synthetic TC events, we generate streamflow simulations initialized

by climate conditions prescribed by corresponding CMIP6 models. For each storm, the prior year of CMIP6 climate (precipitation and temperature) is chosen for spinning up each streamflow simulation. This initial condition is random in the CMIP6 set of simulations because every synthetic storm starts at a different time. It is designed to test how the TCP flood risk changed with the background climate.

### 2.3. Statistical estimation of risk

We estimate the return periods for both the TCP properties (rain rate and storm total TCP) and TC associated stream flows at Whiteoak Bayou and Buffalo Bayou. The very large sample (4500) for each set provides a more robust risk assessment of the very rare extreme events, which may never have been recorded in the past. Here we define the return period as the inverse of the annual exceedance probability. The return periods are estimated for maximum event TCP, maximum TCP rain ratio, and maximum daily streamflow in each set of storms. We use the Poisson distribution to quantify the uncertainties in the estimation of storm frequencies given by the synthetic model at the 90% confidence interval. Here the assumption is that the frequency within each kernel follows a Poisson distribution with the empirical kernel frequency as the mean. The 5% and 95% quantiles of the Poisson distribution are then derived as lower and upper boundaries and 90% of the events would fall between them. The boundary frequencies are remapped into return periods for the 90% confidence interval shadings for individual models. We also collected all empirical frequency/magnitude curves from eight different CMIP6 models and calculate their ensemble mean curves for both historical and SSP5-8.5 scenarios, using linear interpolations. Here we calculated the  $\pm 1$  standard deviation from frequencies of eight models transform them into the uncertainty shading for the ensemble mean estimates of return periods. Both the uncertainty shadings for the individual models and the ensemble mean may reach the value of infinity when the estimated frequency is approaching zero. We compared the ensemble mean risk profiles of TCP and floods from both historical and SSP5-8.5, as well as their variations in different CMIP6 models.

## 3. Results

### 3.1. Change in TCP risk at Houston

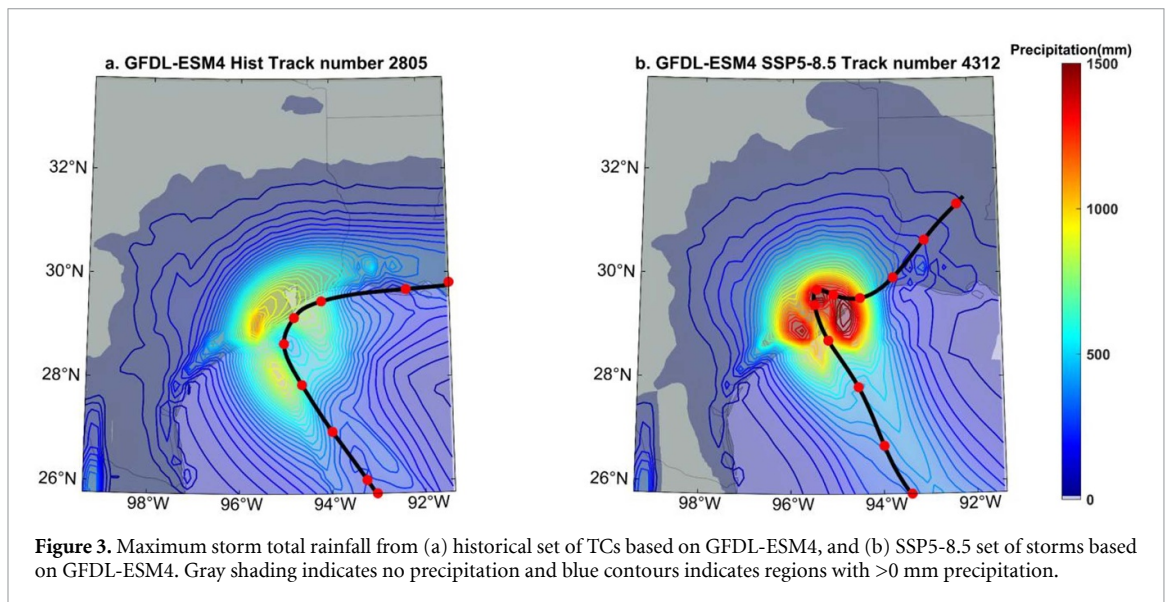
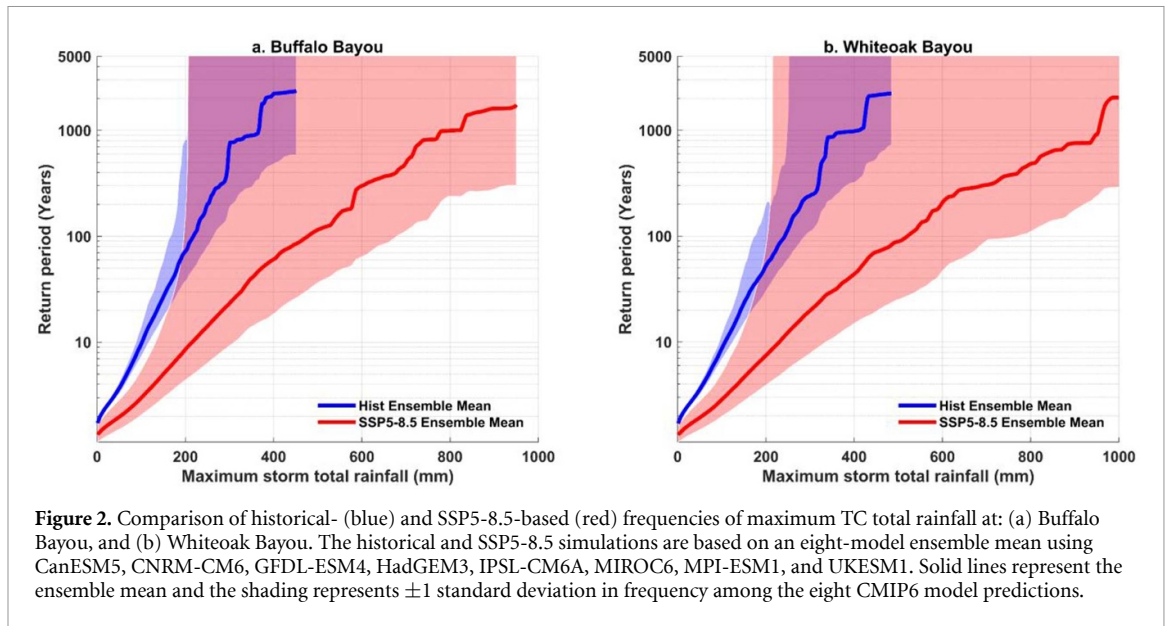
We estimate the frequencies of maximum storm total rainfall for all sets of synthetic TCs from eight CMIP6 models and average their frequencies to produce the probability curves based on historical and SSP5-8.5 ensembles (figure 2). At Buffalo Bayou, the SSP5-8.5 scenarios have a substantial increase of risk in storm total rainfall as compared with the historical scenarios. The maximum value is only 450 mm in the historical ensemble because there are too few synthetic

events above that threshold to make robust estimates of the mean return period for all eight models. Based on estimates from precipitation observations (Di Luzio *et al* 2008), Hurricane Harvey produced  $\sim 780$  mm of precipitation within the Buffalo Bayou watershed in 5 d. Here we conservatively define 450 mm as precipitation of ‘Harvey magnitude’. Buffalo Bayou’s return period of storm total rainfall at this magnitude changes from  $>2000$  years in the historical ensembles to  $<100$  years in the SSP5-8.5 ensembles. There is variability among different model predictions as shown by the uncertainty envelope in figure 2(a) as well as separate comparisons for different models in SI 2. All models show increases in TCP in the SSP5-8.5 scenario as compared to the historical simulations. The largest change of TCP risk is obtained by the IPSL-CM6A, which estimates the return period for the ‘Harvey magnitude’ precipitation will change from  $>5000$  years in the historical simulation to  $<20$  years in the SSP5-8.5 simulation (SI 2(e)). The MPI-ESM1 (SI 2(g)) has the smallest change in the return period for the ‘Harvey magnitude’ precipitation, it decreases from 800 years to 300 years.

The increases in TCP risk in Whiteoak Bayou (figure 2(b)) are similar to Buffalo Bayou, but with a slightly shorter return period for the same magnitude of TCP. For example, the mean return period of 200 mm historical TCP is 50 years for Whiteoak Bayou and 80 years for Buffalo Bayou. The mean return period of 800 mm SSP5-8.5 TCP is 500 years for Whiteoak Bayou and  $>100$  years for Buffalo Bayou. Elevated TCP risk from historical to SSP5-8.5 in Whiteoak Bayou is consistent across all eight climate models (SIs 2 and 3).

Extreme TCs cause substantial property damage and generate catastrophes to society (Lin and Emanuel 2016, Emanuel 2021), so we selected a ‘black swan’ event for each set and compared their spatial patterns (SIs 4 and 5). One case is shown in figure 3 for the most extreme TCP event generated from the historical (figure 3(a)) and SSP5-8.5 (figure 3(b)) scenarios of the GFDL-ESM4.

A drastic increase in precipitation intensity is evident from figure 3(a) to figure 3(b). The historical event has maxima of 1000 mm over the northwestern portion of its rain swath, while the SSP5-8.5 event has maxima of  $>1500$  mm with a more widespread spatial pattern, mostly located over the eastern portion. This difference is related to the different track characteristics of the two extreme TC events. The SSP5-8.5 event (figure 3(b)) has a more curved track, particularly after it makes landfall. More lingering time generates more precipitation over the Houston area. Similar variations are also evident in the most extreme TCP cases generated from the other seven models. Most models have increased precipitation from the historical to the SSP5-8.5 case, with the only exception being MIROC6 (SIs 5(b) and (f)). The maximum



rainfall case for the MIROC6 historical run (SI 5(b)) is a stalled TC like Hurricane Harvey; it has slightly more precipitation than the maximum case for the CMIP6 run (SI 5(f)), which results from its more regular movement. Two storms demonstrate TCP with magnitude  $>5000$  mm from SSP5-8.5 runs: IPSL-6A and the UKESM1 (SIs 5(e) and (h)). This magnitude of TCP has only been reported in TC Gamede at the island of La Réunion over the Indian ocean in February 2007 (Quetelard *et al* 2009). It would be catastrophic if a TC with that amount of precipitation (about six times more than Harvey) impacted densely populated coastal cities like Houston.

Another important feature for those wettest storms is the curvature of their tracks. Historically, many storms that produced massive precipitation in TX are ‘stalled’ systems like Tropical Storm Allison in 2001 and Hurricane Harvey in 2017. Stalled TCs

are likely to generate more precipitation because they linger at one location or affect the same location twice (Hall and Kossin 2019). Many storm tracks (figure 3, SIs 4 and 5) resemble Harvey’s track, which heads towards the northwest first, slows down as it makes landfall and moves very slowly, and finally heads out in the opposite direction (east).

### 3.2. Factors contributing to change in TCP risk

Part of the elevated risk of storm total rainfall arises from changes in storm tracks. We already showed that many of the wettest storms have very slow translation speed and curved tracks when approaching Houston. Here we compare how the translation speed of all simulated storms changes in this region in the SSP5-8.5 runs. Figure 4(a) shows that the frequency distribution of the translation speed systematically shifts toward smaller values in the SSP5-8.5 runs. The

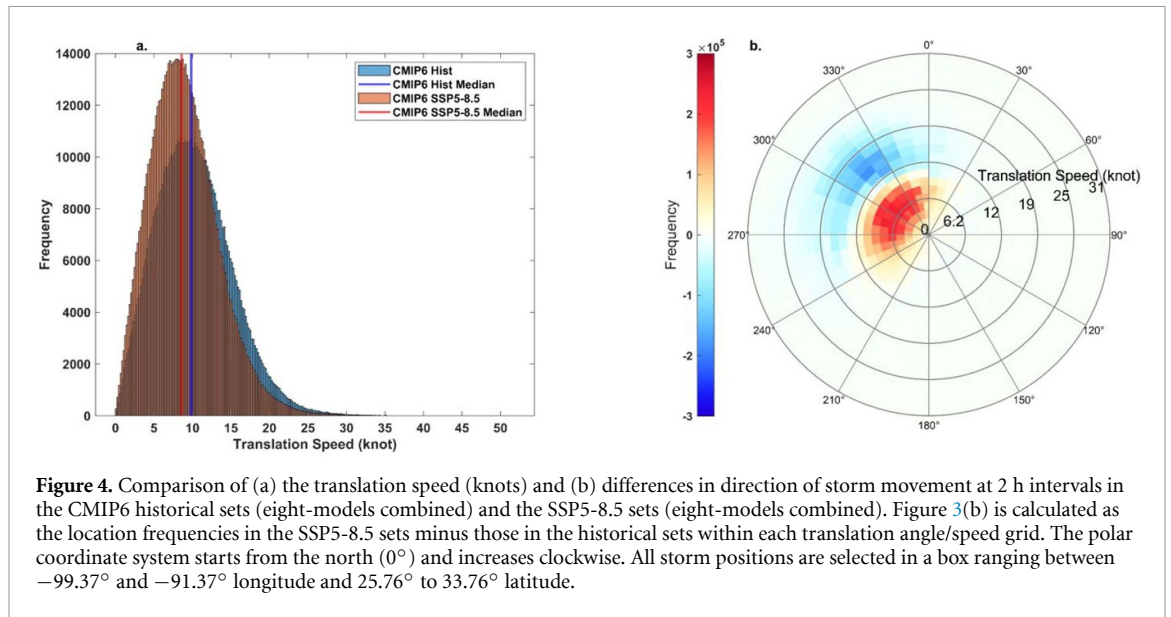


**Figure 4.** Comparison of (a) the translation speed (knots) and (b) differences in direction of storm movement at 2 h intervals in the CMIP6 historical sets (eight-models combined) and the SSP5-8.5 sets (eight-models combined). Figure 3(b) is calculated as the location frequencies in the SSP5-8.5 sets minus those in the historical sets within each translation angle/speed grid. The polar coordinate system starts from the north ( $0^\circ$ ) and increases clockwise. All storm positions are selected in a box ranging between  $-99.37^\circ$  and  $-91.37^\circ$  longitude and  $25.76^\circ$  to  $33.76^\circ$  latitude.

median translation speed (red) is 8.42 knots for SSP5-8.5 storms as compared to 9.86 knots (blue) for historical storms, a 17% reduction. SSP5-8.5 also indicates more frequent landfall of TCs within 500 km of Houston. Figure 4(b) shows the frequency difference rose of storm translation directions and speed for both scenarios. The SSP5-8.5 sets have higher frequencies of slower moving storms ( $<11$  knots) and lower frequencies of faster storms ( $>11$  knots) as compared with the historical sets. In particular, SSP5-8.5 shows an increase in the frequencies of storms that move towards the south at slower translation speeds. Our results indicate that storms in this region are more likely to move slower and to stall, which has been observed both globally (Kossin 2018) and regionally (Hall and Kossin 2019, Hassanzadeh *et al* 2020). Changes in storm translation angle and speed in different models (SI 6) are generally consistent with the patterns in figure 4(b). Many demonstrate a slowing down of SSP5-8.5 storms and more frequent southward movement. The MPI-ESM1 is the exception and it shows increased northward movement and reduced southward movement of storms in SSP5-8.5. This may result from MPI-ESM1's different representation of general circulation patterns from other models.

Higher rain ratios constitute another physical mechanism for elevated risk in storm total rainfall in SSP5-8.5 runs. Based on the Clausius–Clapeyron equation, higher air temperatures enable the atmosphere to contain more moisture, which may intensify precipitation extremes in a warming world (Trenberth *et al* 2003, O’Gorman and Schneider 2009). Ensemble means (figure 5) of the hourly rain rate show that TCs in the SSP5-8.5 climate scenario have higher probabilities of extreme hourly rain rates than the historical scenario. According to NOAA (Blake and Zelinsky 2017), the most extreme

hourly rain rate observed in Harvey was  $173 \text{ mm h}^{-1}$  and many areas near Houston observed a maximum hourly rain ratio of  $50\text{--}75 \text{ mm h}^{-1}$ .

It is the maximum magnitude that our historical ensemble mean can yield a robust estimate for a 1500 year return period for both Buffalo Bayou (SI 7) and Whiteoak Bayou (SI 8). The return periods for the same magnitude of TC rain rate reduce to only  $\sim 150$  years in the SSP5-8.5 ensemble means. Different models also demonstrate variations in TC rain rate probability, but all show an elevated probability in a warmer climate (SIs 7 and 8). Whiteoak Bayou has a slightly higher probability of rain rate than Buffalo Bayou. For example, the return period of  $110 \text{ mm h}^{-1}$  SSP5-8.5 rain rate is  $>700$  years for Buffalo Bayou, but only 500 years for Whiteoak Bayou.

### 3.3. Change in TC pluvial flood risk

To understand how flood risk changes with TCP magnitude, we calibrate the AirGR GR4J hydrological model (Perrin *et al* 2003) for both Buffalo Bayou and Whiteoak Bayou and coupled our synthetic TCP events with them (see section 2 for details). Figure 6 displays comparisons between historical and SSP5-8.5 TCP-driven daily maximum daily stream flows. Both watersheds have significantly elevated TCP flood probability from the historical ensemble to the SSP5-8.5 ensemble, but they have quite different patterns. Observed maximum daily streamflow is  $\sim 390 \text{ m}^3 \text{ s}^{-1}$  for the Buffalo Bayou and  $\sim 1160 \text{ m}^3 \text{ s}^{-1}$  for the Whiteoak Bayou from the USGS record (figure 1), both maxima were associated with Hurricane Harvey.

The historical ensemble means (blue curves) give more conservative estimates of return periods for the maximum streamflow at  $\sim 170 \text{ m}^3 \text{ s}^{-1}$  for Buffalo Bayou (figure 6(a)) and  $\sim 430 \text{ m}^3 \text{ s}^{-1}$  for Whiteoak Bayou (figure 6(b)). Buffalo Bayou's  $\sim 170 \text{ m}^3 \text{ s}^{-1}$

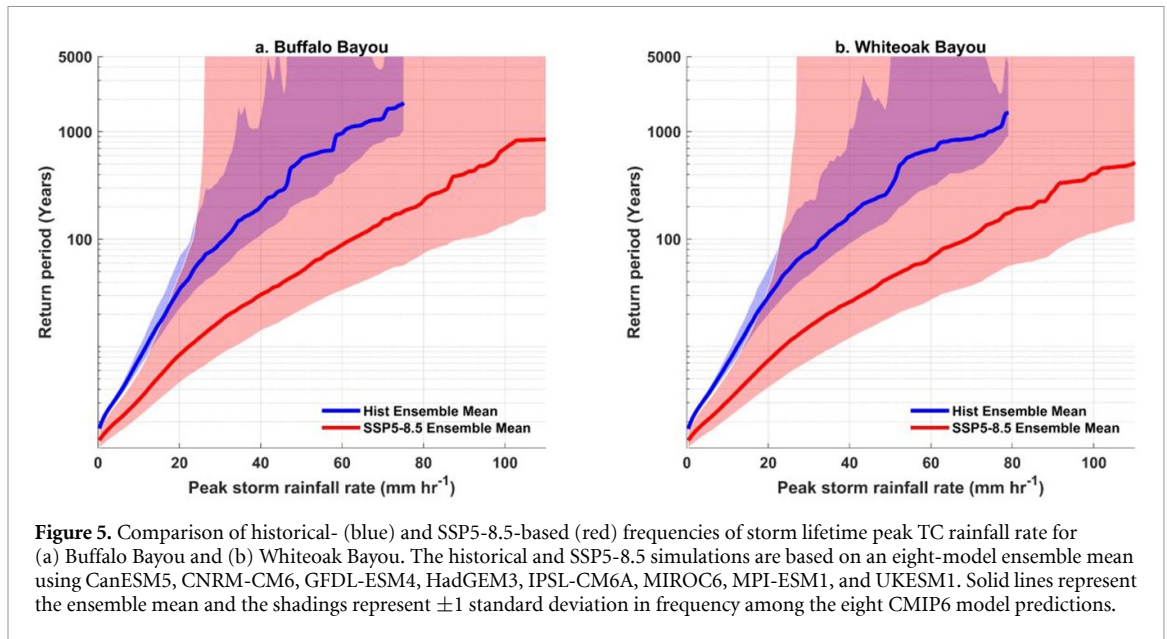


**Figure 5.** Comparison of historical- (blue) and SSP5-8.5-based (red) frequencies of storm lifetime peak TC rainfall rate for (a) Buffalo Bayou and (b) Whiteoak Bayou. The historical and SSP5-8.5 simulations are based on an eight-model ensemble mean using CanESM5, CNRM-CM6, GFDL-ESM4, HadGEM3, IPSL-CM6A, MIROC6, MPI-ESM1, and UKESM1. Solid lines represent the ensemble mean and the shadings represent  $\pm 1$  standard deviation in frequency among the eight CMIP6 model predictions.

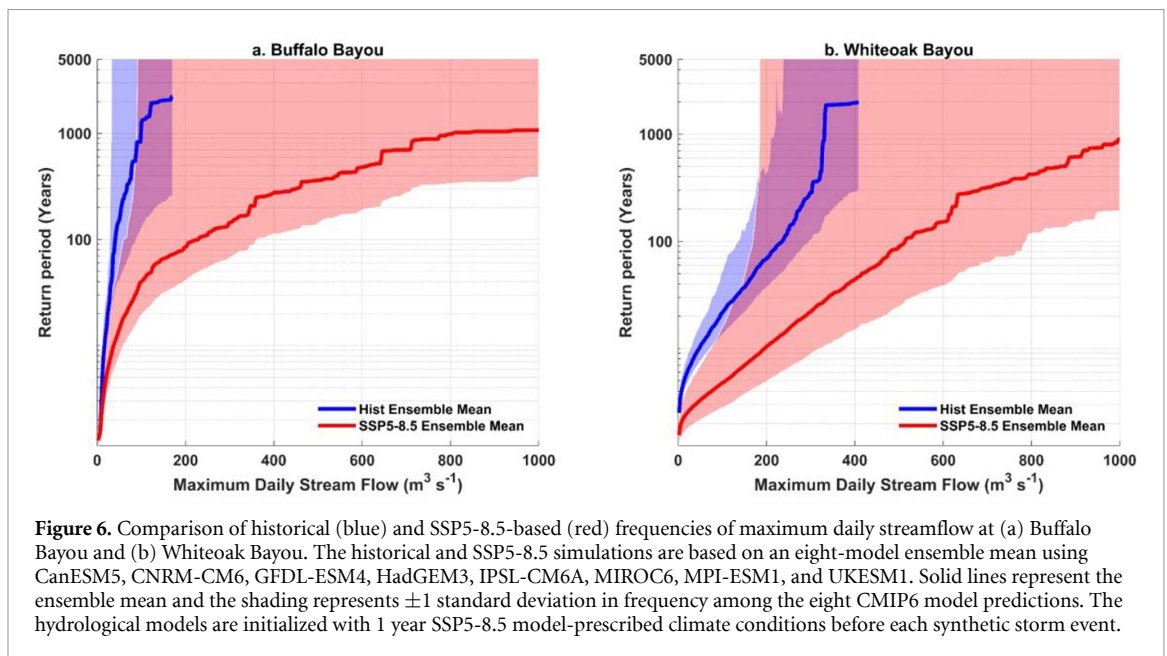


**Figure 6.** Comparison of historical (blue) and SSP5-8.5-based (red) frequencies of maximum daily streamflow at (a) Buffalo Bayou and (b) Whiteoak Bayou. The historical and SSP5-8.5 simulations are based on an eight-model ensemble mean using CanESM5, CNRM-CM6, GFDL-ESM4, HadGEM3, IPSL-CM6A, MIROC6, MPI-ESM1, and UKESM1. Solid lines represent the ensemble mean and the shading represents  $\pm 1$  standard deviation in frequency among the eight CMIP6 model predictions. The hydrological models are initialized with 1 year SSP5-8.5 model-prescribed climate conditions before each synthetic storm event.

return period reduces from 2000 years in the historical ensemble to 60 years in the SSP5-8.5 ensemble. There are even larger changes in Whiteoak Bayou. The return period of the most extreme TCP flood ( $\sim 430 \text{ m}^3 \text{ s}^{-1}$ ) changes from 2000 years in the historical ensemble to  $< 50$  years in the SSP5-8.5 ensemble. The Buffalo Bayou flood probability increases rapidly at a lower magnitude ( $< 250 \text{ m}^3 \text{ s}^{-1}$ ) but starts to flatten at higher magnitudes (figure 6(a)), while the flood probability in Whiteoak Bayou increases more consistently across all magnitudes (figure 6(b)). The CMIP6 models all agree that there will be an elevated TCP flood risk from the historical scenario to the SSP5-8.5 scenario, but they differ in their patterns (SIs 9 and 10). The IPSL-CM6A (SIs 9(e) and 10(e)) has the largest difference in probability between the

historical and SSP5-8.5, while the MPI-ESM1 has the smallest difference.

#### 4. Conclusions

In conclusion, we discover a substantial (1900%) increase in the risk of ‘Harvey Magnitude’ (450 mm) storm rainfall in Houston from the historical ensemble to the SSP5-8.5 ensemble based on large samples of downscaled events from eight CMIP6 models. Different CMIP6 models all agree on the shortening of return periods under climate warming, but variations exist in their magnitudes. This agrees with the previous estimate based on CMIP5 models (Emanuel 2017). Globally, the TC rain rate will have an average of increase of 14% with a range between

6% to 22%, based on 16 different CMIP5 downscaled models and high resolution global models (Knutson *et al* 2020). Previous studies based on multiple models (Risser and Wehner 2017, van Oldenborgh *et al* 2017, Wang *et al* 2018) suggested that Hurricane Harvey's precipitation has likely increased by 8%–38% (most likely 20%) from the historical baseline. Precipitation from the most extreme TCs increases by more than 50% in the majority of our models. Many future TCs will be able to produce >1500 mm precipitation in most downscaled CMIP6 models and can even exceed 5000 mm in rare events. Our results indicate much larger values than the theoretical limit of a 7% increase in saturation specific humidity from a 1 °C increase in the ocean temperature (Stone *et al* 2019, Wehner and Sampson 2021). In addition to the projected significant increases in TC rain rate, our results also indicate that the elevated storm total rainfall is also caused by reduced storm translation speed (17% reduction in the median) and more frequent stalled events in the future. A general decrease in TC translation speed has been observed globally (Kossin 2018) and North Atlantic TCs are more likely to stall in recent years (Hall and Kossin 2019), how they might change in the future and how their rainfall will change needs more investigations.

We observe an even more drastic increase (by a factor of 4000%) in TCP flood risk of Harvey's magnitude from the historical ensemble to the SSP5-8.5 ensemble. The amount of TCP directly determines the risk of flood magnitude, as shown by the ensemble mean and individual CMIP6 models. Buffalo Bayou is a larger watershed with several control structures (Addicks and Baker reservoirs) and more vegetation, while Whiteoak Bayou is a highly urbanized watershed with a smaller size. Therefore, Whiteoak Bayou's hydrological response is much faster and results in a larger magnitude of floods than Buffalo Bayou when they experience similar extreme TCP events because urbanization increases the amount of impervious surfaces and generates faster surface runoff (Zhu *et al* 2015). The TCP flood magnitude also varied based on the antecedent precipitation amount, soil type, watershed size, land use/cover, and engineering flood controls (Sebastian *et al* 2019, Li *et al* 2020). Our analysis based on two watersheds shows that smaller and more intensely urbanized watersheds are at higher risk in future TCP-driven fluvial floods. This agrees with the historical simulation results of Sebastian *et al* (2019), which showed that human development has increased Houston region's peak discharge by 54%, with climate change responsible for 20% of this increase. Population growth and development in this region may exacerbate future TCP flood risk.

Our work strongly suggests that the risk of extreme TCP and resulting flood in Houston will increase substantially in a warming world with no serious attempts to curtail greenhouse gas emissions. Governments and local stakeholders need to come up

with serious mitigation and adaptation to reduce the risk of catastrophes like Hurricane Harvey, which are likely to increase as the planet continues to warm.

## Data availability statement

The data that support the findings of this study are available upon reasonable request from the authors.

## Acknowledgments

LZ is supported by the Faculty Start-up Funding and the Harrison Endowment Funding by the Department of Geography, Environment, and Tourism, Western Michigan University. KE is supported by NSF Grant ICER-1854929.

## Author contributions

KE designed the SDT and TCR algorithms; LZ conceptualized the research and designed the experiments of hydrological simulations. LZ drafted the manuscript, with discussions and contributions from SQ and KE.

## Conflict of interest

The authors declare no competing interests.

## ORCID iD

Laiyin Zhu  <https://orcid.org/0000-0003-3612-7583>

## References

- Blake E S and Zelinsky D A 2017 National Hurricane center tropical cyclone report Hurricane Harvey
- Davis C A 2018 Resolving tropical cyclone intensity in models *Geophys. Res. Lett.* **45** 2082–7
- Di Luzio M, Johnson G L, Daly C, Eischeid J K and Arnold J G 2008 Constructing retrospective gridded daily precipitation and temperature datasets for the conterminous United States *J. Appl. Meteorol. Climatol.* **47** 475–97
- Emanuel K A 2013 Downscaling CMIP5 climate models shows increased tropical cyclone activity over the 21st century *Proc. Natl Acad. Sci.* **110** 12219–24
- Emanuel K 2017 Assessing the present and future probability of Hurricane Harvey's rainfall *Proc. Natl Acad. Sci.* **114** 12681–4
- Emanuel K 2021 Response of global tropical cyclone activity to increasing CO<sub>2</sub>: results from downscaling CMIP6 models *J. Clim.* **34** 57–70
- Emanuel K, Ravela S, Vivant E and Risi C 2006 A statistical deterministic approach to Hurricane risk assessment *Bull. Am. Meteorol. Soc.* **87** 299–314
- Emanuel K, Sundararajan R and Williams J 2008 Hurricanes and global warming: results from downscaling IPCC AR4 simulations *Bull. Am. Meteorol. Soc.* **89** 347–68
- ESRI 2020a 'Dark gray canvas' [locator map]. Scale not given *Dark Gray Canvas* (available at: [www.arcgis.com/home/item.html?id=1970c1995b8f44749f4b9b6e81b5ba45](http://www.arcgis.com/home/item.html?id=1970c1995b8f44749f4b9b6e81b5ba45))
- ESRI 2020b 'National' [basemap]. Scale not given *USGS National Map* (available at: [www.arcgis.com/home/item.html?id=6d9fa6d159ae4a1f80b9e296ed300767](http://www.arcgis.com/home/item.html?id=6d9fa6d159ae4a1f80b9e296ed300767))

- Feldmann M, Emanuel K, Zhu L and Lohmann U 2019 Estimation of Atlantic tropical cyclone rainfall frequency in the United States *J. Appl. Meteorol. Climatol.* **58** 1853–66
- Ficchi A, Perrin C and Andréassian V 2019 Hydrological modelling at multiple sub-daily time steps: model improvement via flux-matching *J. Hydrol.* **575** 1308–27
- Gutmann E D, Rasmussen R M, Liu C, Ikeda K, Bruyere C L, Done J M, Garrè L, Friis-Hansen P and Veldore V 2018 Changes in Hurricanes from a 13 yr convection-permitting pseudo-global warming simulation *J. Clim.* **31** 3643–57
- Hall T M and Kossin J P 2019 Hurricane stalling along the North American coast and implications for rainfall *npj Clim. Atmos. Sci.* **2** 17
- Hassanzadeh P, Lee C-Y, Nabizadeh E, Camargo S J, Ma D and Yeung L Y 2020 Effects of climate change on the movement of future landfalling TX tropical cyclones *Nat. Commun.* **11** 3319
- Irvine P, Emanuel K, He J, Horowitz L W, Vecchi G and Keith D 2019 Halving warming with idealized solar geoengineering moderates key climate hazards *Nat. Clim. Change* **9** 295–9
- Knutson T R, Sirutis J J, Vecchi G A, Garner S, Zhao M, Kim H-S, Bender M, Tuleya R E, Held I M and Villarini G 2013 Dynamical downscaling projections of 21st-century Atlantic Hurricane activity: CMIP3 and CMIP5 model-based scenarios *J. Clim.* **26** 6591–617
- Knutson T R, Sirutis J J, Zhao M, Tuleya R E, Bender M, Vecchi G A, Villarini G and Chavas D 2015 Global projections of intense tropical cyclone activity for the late 21st century from dynamical downscaling of CMIP5/RCP4.5 scenarios *J. Clim.* **28** 7203–24
- Knutson T et al 2020 Tropical cyclones and climate change assessment: part II: projected response to anthropogenic warming *Bull. Am. Meteorol. Soc.* **101** E303–E22
- Kossin J P 2018 A global slowdown of tropical-cyclone translation speed *Nature* **558** 104–7
- Li X, Zhao G, Nielsen-Gammon J, Salazar J, Wigmosta M, Sun N, Judi D and Gao H 2020 Impacts of urbanization, antecedent rainfall event, and cyclone tracks on extreme floods at Houston reservoirs during Hurricane Harvey *Environ. Res. Lett.* **15** 124012
- Lin N and Emanuel K 2016 Grey swan tropical cyclones *Nat. Clim. Change* **6** 106–11
- Lu P, Lin N, Emanuel K, Chavas D and Smith J 2018 Assessing Hurricane rainfall mechanisms using a physics-based model: Hurricanes Isabel (2003) and Irene (2011) *J. Atmos. Sci.* **75** 2337–58
- Michaelis A C and Lackmann G M 2019 Climatological changes in the extratropical transition of tropical cyclones in high-resolution global simulations *J. Clim.* **32** 8733–53
- NOAA 2021 National centers for environmental information (NCEI) US Billion-Dollar Weather and Climate Disasters
- O’Gorman P A and Schneider T 2009 The physical basis for increases in precipitation extremes in simulations of 21st-century climate change *Proc. Natl Acad. Sci.* **106** 14773–7
- Olivera F and Defee B B 2007 Urbanization and its effect on runoff in the Whiteoak Bayou watershed, TX1 *J. Am. Water Resour. Assoc.* **43** 170–82
- Oudin L, Salavati B, Furusho-Percot C, Ribstein P and Saadi M 2018 Hydrological impacts of urbanization at the catchment scale *J. Hydrol.* **559** 774–86
- Patricola C M and Wehner M F 2018 Anthropogenic influences on major tropical cyclone events *Nature* **563** 339–46
- Perrin C, Michel C and Andréassian V 2003 Improvement of a parsimonious model for streamflow simulation *J. Hydrol.* **279** 275–89
- Quetelard H, Bessemoulin P, Cerveny R S, Peterson T C, Burton A and Boodhoo Y 2009 Extreme weather: world-record rainfalls during tropical cyclone game *Bull. Am. Meteorol. Soc.* **90** 603–8
- Risser M D and Wehner M F 2017 Attributable human-induced changes in the likelihood and magnitude of the observed extreme precipitation during Hurricane Harvey *Geophys. Res. Lett.* **44** 12457–464
- Salas J D and Obeysekera J 2014 Revisiting the concepts of return period and risk for nonstationary hydrologic extreme events *J. Hydrol. Eng.* **19** 554–68
- Sebastian A, Gori A, Blessing R B, van der Wiel K and Bass B 2019 Disentangling the impacts of human and environmental change on catchment response during Hurricane Harvey *Environ. Res. Lett.* **14** 124023
- Stone D A et al 2019 Experiment design of the International CLIVAR C20C+ detection and attribution project *Weather Clim. Extremes* **24** 100206
- Trenberth K E, Dai A, Rasmussen R M and Parsons D B 2003 The changing character of precipitation *Bull. Am. Meteorol. Soc.* **84** 1205–18
- van Oldenborgh G J, van der Wiel K, Sebastian A, Singh R, Arrighi J, Otto F, Haustein K, Li S, Vecchi G and Cullen H 2017 Attribution of extreme rainfall from Hurricane Harvey, August 2017 *Environ. Res. Lett.* **12** 124009
- Villarini G, Lavers D A, Scoccimarro E, Zhao M, Wehner M F, Vecchi G A, Knutson T R and Reed K A 2014 Sensitivity of tropical cyclone rainfall to idealized global-scale forcings\* *J. Clim.* **27** 4622–41
- Wang S Y S, Zhao L, Yoon J-H, Klotzbach P and Gillies R R 2018 Quantitative attribution of climate effects on Hurricane Harvey’s extreme rainfall in TX *Environ. Res. Lett.* **13** 054014
- Wehner M F et al 2014 The effect of horizontal resolution on simulation quality in the community atmospheric model, CAM5.1 *J. Adv. Model. Earth Syst.* **6** 980–97
- Wehner M and Sampson C 2021 Attributable human-induced changes in the magnitude of flooding in the Houston, TX region during Hurricane Harvey *Clim. Change* **166** 20
- Xi D, Lin N and Smith J 2020 Evaluation of a physics-based tropical cyclone rainfall model for risk assessment *J. Hydrometeorol.* **21** 2197–218
- Yoshida K, Sugi M, Mizuta R, Murakami H and Ishii M 2017 Future changes in tropical cyclone activity in high-resolution large-ensemble simulations *Geophys. Res. Lett.* **44** 9910–7
- Zhang W, Villarini G, Vecchi G A and Smith J A 2018 Urbanization exacerbated the rainfall and flooding caused by Hurricane Harvey in Houston *Nature* **563** 384–8
- Zhu L, Quiring S M and Emanuel K A 2013 Estimating tropical cyclone precipitation risk in TX *Geophys. Res. Lett.* **40** 6225–30
- Zhu L, Quiring S M, Gonalp I and Peacock W G 2015 Variations in tropical cyclone-related discharge in four watersheds near Houston, TX *Clim. Risk Manage.* **7** 1–10